Biophysical Chemistry 8 (1978) 41–51

A UNIFIED THEORY OF NUCLEATION-RATE-LIMITED DNA RENATURATION KINETICS

Donald C. RAU and Lynn C. KLOTZ*
Department of Biochemistry and Molecular Biology, Harvard University, Cambridge, Massachusetts 02138, USA

Received 12 May 1977

DNA renaturations under nucleation-rate-limiting conditions on simple DNA such as bacterial and bacteriophage DNA show significant deviation from ideal second-order kinetics when followed by optical density measurements at 260 nm. Ideal second-order kinetics yield linear plots when the data is plotted in the standard reciprocal second-order (RSO) manner. The observed deviations from ideal second-order behavior take the form of steadily downward-curving RSO plots. In this paper, experiments are presented for E. coli and T2 DNA documenting this non-ideal behavior. Since experiments using T4, T5 and B. subtilis DNA yield identical non-ideal behavior, this behavior appears to be a property of DNA renaturation followed by optical density, not a peculiarity of a particular DNA. Identical non-ideal behavior is also seen in kinetics followed by S1 nuclease assay. A theory is developed to explain this deviation from ideal second-order kinetics. The theory also explains why kinetics followed by hydroxyapatite chromatography show nearly ideal second-order kinetics. In contrast to the approach taken by others in developing equations that describe S1 nuclease monitored reactions, our view is that non-ideal second-order kinetics are fundamentally due to the reaction of free single strands to yield partially helical duplex species. Later reactions of these species tend to reduce the deviations from non-ideal second-order kinetics.

1. Introduction

With the increasing importance of DNA renaturation as a tool for the investigation of eucaryotic DNA sequences, physical studies on the kinetics of renaturation provide a necessary foundation for the analysis of experimental data. Basically, there are two classes of techniques for monitoring the extent of a renaturation reaction. One can follow either the time course of reaction of whole free single strands as with hydroxyapatite, or the extent of reaction of base pairs as with S1 nuclease and optical methods.

For reactions that are ideally second-order, i.e., $2A \xrightarrow{k_2} B$, experimental kinetic data will be linearized when graphed as prescribed by the standard second-order relationship, $A_0/A(t) - 1$ versus time, where $A(t)/A_0$ is the fraction unreacted. In this paper, we shall refer to such plots as RSO (Reciprocal-Second-Order) plots.

For renaturation reactions of simple DNA (i.e., DNA which behaves as if it were a single kinetic class) such as bacterial or bacteriophage DNA monitored by hydroxyapatite, it has been reported [1,2] that the kinetic time course of reaction closely follows ideal second-order behavior; that is, RSO plots are linear. Recently, however, significant deviations from ideal second-order kinetics have been reported from reactions monitored with S1 nuclease [2,3]. Rather than resulting in a straight line, experimental data obtained with S1 nuclease yields steadily downward curving RSO plots. For kinetics followed by optical density, downward curving RSO plots identical to those followed with S1 nuclease are observed under many experimental conditions (data presented here). Downward curvature in optically monitored renaturations has been observed by others also [4,5].

Since the S1 nuclease and the optical hypochromicity methods monitor the extent of base pair reaction, both techniques should result in equivalent kinetics. On the other hand, hydroxyapatite monitors two-stranded molecules regardless of how many base pairs have formed, so the time course of the kinetics may be expected to differ from those followed by S1 nuclease or optical density. We present here a simple,

* To whom reprint requests should be addressed.

ideal theory for nucleation-rate-limited DNA renaturation kinetics which explains the different observed types of RSO plots. The assumptions of this ideal theory are exactly those of Wetmur and Davidson [6], but we obtain a different final result. Modifications of the theory to make it correspond more closely to real experiments are discussed. Results are presented for optical density monitored experiments on T2 and E. coli DNA.

2. Ideal kinetic theory

To derive the theory, we take a very simple case:

(1) Let all the single strands be the same length L.

(2) Assume also that the kinetics are nucleation rate limiting; that is, the rate at which the strands collide to form the first few base pairs (nucleation) is small compared to the rate at which the base pairs zip to form the maximum number of pairs. Zipping is instantaneous.

(3) We assume that the single stranded DNA has been prepared by some method of random shearing of double-stranded DNA such as mechanical breakage using a sonicator, homogenizer or French press. These are standard methods of preparing sheared DNA. Under conditions where the single strands have been prepared by such extensive random shearing, the two fully zipped strands will only be partially complementary to each other. Assuming that the probability of the existence of an i-base paired species is proportional to i, Wetmur [7] showed that, on the average, $\frac{2}{3}L$ base pairs zip when all strands have length L. This situation is illustrated in panel B of fig. 1.

(4) For the present, we assume that three-stranded partially base-paired species (panel C) and concatemers (panel D) do not form: that is, the single-stranded ends of two stranded partially base-paired species are totally unreactive.

We will take into account later the effect on the kinetics of the reaction of the single strand ends of partially base-paired species and the effect of single strands having a distribution of lengths instead of a single length, L.

To describe the time course of the reaction, the following symbols and relationships are used.

t Time.

α Average fraction of base pairs zipped in the reaction of free single strands.

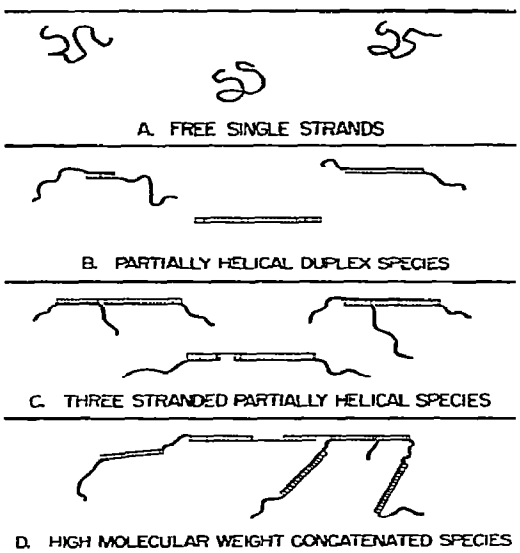

Fig. 1. A schematic representation of the renaturation reaction of DNA single strands with a random distribution of partially overlapping sequences. Panel A represents the initial population of denatured single strands. The reaction of two single strands will yield a population of partially helical duplexes represented in panel B. The reaction of the tails of partially helical duplexes with free single strands or with each other will give such products as those depicted in panel C. Panel D shows some typical concatemers that will be formed after about 60% reaction.

k_2 The second-order rate constant for nucleation of free single strands of length L nucleotides.

R_0 The concentration of free (+) single strands of time $t = 0$. In common practice, this is also the concentration of free (−) single strands at time $t = 0$.

$R(t)$ The concentration of free (+) single strands at time t. $R(t)$ is also the concentration of free (−) single strands at time t.

$S(t)$ The concentration of partially helical duplex species at time t. Since each duplex is composed of one (+) strand and one (−) strand, $R_0 = R(t) + S(t)$.

A_0 The concentration of nonhelical base pairs at time $t = 0$. In terms of strands, $A_0 = LR_0$.

$A(t)$ The concentration of nonhelical base pairs at time t. If the zipping reaction of the αL base pairs of a nucleated duplex is instantaneous, then $A(t) = A_0 - \alpha LS(t)$.

For the second order nucleation reaction of free (+) and (−) single strands, the standard kinetic equation can be written,

$$-\mathrm{d}R(t)/\mathrm{d}T = \mathrm{d}S(t)/\mathrm{d}T = k_2(R(t))^2. \quad (1)$$

From the relationship between R_0, $S(t)$, and $R(t)$, (1) can be written as,

$$\mathrm{d}S(t)/\mathrm{d}T = k_2(R_0 - S(t))^2. \quad (2)$$

Straight forward integration gives the standard second-order equation,

$$1/(R_0 - S(t)) - 1/R_0 = k_2 t. \quad (3)$$

Since partially helical duplex species, however, contain both helical and nonhelical base pairs, if eq. (3) is now cast in terms of nonhelical base pair concentrations (with the substitutions, $R_0 = A_0/L$ and $S(t) = (A_0 - A(t))/\alpha L$), there results the following non standard second-order form,

$$\frac{\alpha A_0}{A(t) - (1-\alpha)A_0} - 1 = k_2' A_0 t, \quad (4)$$

where $k_2/L = k_2'$, the nucleation rate constant per molar nucleotides. Eq. (4) can be algebraically manipulated to give the RSO plot form,

$$\frac{A_0}{A(t)} - 1 = \frac{\alpha k_2' A_0 t}{1 + (1-\alpha)k_2' A_0 t}. \quad (5)$$

Even though this equation is the result of a derivation for an ideal case, it is worthwhile here to discuss some points concerning it. For reactions followed by optical density or S1 nuclease where the concentration of base pairs is monitored, eq. (5) predicts the results of an ideal experiment. As time, t, increases the denominator increases, so that the equation predicts downward curving RSO plots as observed in real experiments [2–5]. In fact, even the degree of curvature in real experiments for the first 40% of reaction (see below), is well-described by the ideal $\alpha = \frac{2}{3}$. For kinetics followed by hydroxyapatite chromatography, all nucleotides whether they are base-paired or on single-strand ends are counted equally. This is equivalent to setting $\alpha = 1$ in eq. (5) yielding the standard second-order form

$$A_0/A(t) - 1 = k_2' A_0 t. \quad (6)$$

Linear RSO plots of hydroxyapatite monitored experiments on simple DNA are routinely observed, at least for the first 40% of reaction [1, 2, 8]. While the difference between hydroxyapatite monitored and optical density or S1 monitored renaturations is explained by the theory, the almost exact agreement with the ideal theory is somewhat fortuitous (see discussion).

For $\alpha \neq 1$, it should further be noted that although standard RSO plots are not linear, rates of reactions determined either from initial slopes of RSO plots or from half times of reaction do exhibit simple second-order concentration dependence.

The theory also predicts that the renaturation kinetics of perfectly complementary DNA, such as fragments prepared using restriction enzymes, should follow eq. (6) since $\alpha = 1$ in this case. Renaturation kinetics on restriction fragments monitored with S1 nuclease do yield linear RSO plots [3].

Our theory has been derived under the same set of assumptions as the Wetmur and Davidson theory [6]. Our result, eq. (5), differs from their theoretical result that optical renaturations follow a second-order time course as described by eq. (6). The difference is in the way we and they have taken into account the factor α for partially base-paired species. We assume that *single strands* nucleate with second-order kinetics, and the factor α enters the theory when the strands then zip instantaneously. That is, α is used to convert the concentration of nucleated strands $S(t)$ to concentrations of base pairs formed, $A_0 - A(t) = \alpha L S(t)$. In a sense, the mathematics follows the physics of renaturation. In the Wetmur and Davidson theory, they start by assuming that individual *nucleotides* nucleate with second-order kinetics, and thus obtain eq. (6). They take into account the factor α only in the rate constant by multiplying the second-order constant, k_2', by α; i.e., only $\frac{2}{3}$ of the nucleotides on any strand can nucleate. This is physically equivalent to a reaction in which the single strands have length $\frac{2}{3}L$ and are completely complementary (such as restriction fragments). We believe this is incorrect for optically monitored reactions on randomly sheared DNA.

Another way to look at downward curvature is that many researchers take the optical density of native DNA as the infinite-time optical density, OD(∞), when analyzing renaturation kinetic data, so that the total extent of reaction is OD(0) − OD(∞), where OD(0) is the denatured optical density. Instead, they should be taking $\frac{2}{3}$ [OD(0) − OD(∞)] for the ideal case. In other words, for the ideal case where the free single

strand ends of two-stranded species are unreactive, at infinite time, $\frac{1}{3}$ of the nucleotides remain unreacted. These considerations allow one to construct eq. (4) directly. Clearly, this view must be modified somewhat to account for the reaction of the single strand ends (see discussion). Nevertheless, eqs. (4) and (5) are valid at early times in the reaction when three-stranded species and concatemers do not form.

When analyzing experimental results, it is convenient to have a parameter which measures degree of curvature in RSO plots. We define a parameter p as follows

$$\frac{A_0}{A(t)} - 1 = \frac{p\,k_2' A_0 t}{1 + (1-p)\,k_2' A_0 t}. \qquad (7)$$

This equation is the same as eq. (5) except that p has replaced α. Thus, p is now an empirical parameter to described RSO curvature: $p = 1$ implies no curvature and smaller p values mean greater curvature.

Before considering theoretical modifications for non-ideal kinetics, it is necessary to analyze in detail the time course of optically monitored renaturation kinetics of simple DNA under nucleation-rate-limiting conditions.

3. Materials and methods

3.1. Preparation and extraction of E. coli and T2 DNA

E. coli B cells were grown in an M 9 salts medium [18] supplemented with 50 mg/ml $CaCl_2$, 140 mg/ml L-tryptophan, 20 mg/ml thymine, 340 mg/ml L-arginine, 300 mg/ml L-methionine, and 2% dextrose. Prior to the inoculation of this liquid with E. coli B cells, a fresh tryptose blood agar slant was inoculated from stock slants of E. coli B and incubated overnight at 37°C. The supplemented M 9 salts medium was then inoculated from this slant. The cells were incubated at 37°C and aerated by shaking. The cells were allowed to grow 4–8 hours into stationary phase (16–20 hours total incubation time), then harvested by low speed (5000 rpm) centrifugation. E. coli DNA was then isolated and purified by the standard procedure of Marmur [9]. Whole T2 phage was purchased from Miles Laboratories, Inc. The DNA was isolated and purified by successive phenol (chromatography grade) extractions [10]. Isolated DNA was then dialyzed against a large excess of 1 X SSC, with several changes of buffer.

The purity of the dialyzed native DNA was checked against several criteria. The ratio of absorbances at 260 nm and 280 nm had to be at least 1.8; while the ratio of absorbances at 260 nm and 230 nm had to be at least 2.1. The absorbance-temperature profiles at 260 nm (melting curves) were obtained using an Automatic Recording Gilford Spectrophotometer, Model 2000, equipped with an automatic reference compensator and linear temperature programmer. Melting profiles were checked for the melting temperature of transition (T_m), steepness of transition (a melting half-bredth of, at maximum, 3°C), and cooperativity of transition, i.e., absorbance profiles well below the T_m were examined for the non-cooperative melting of single stranded DNA and RNA. In all cases, the hyperchromicity of native, unsheared DNA was about (0.36 ± 0.01) ((OD *melted* − OD *native*)/OD *native*). The melting profiles of the phage DNA showed no observable contamination by host E. coli DNA.

3.2. DNA concentrations

Chemical determinations of DNA concentrations were determined by a diaminobenzoic acid fluorescence assay [11]. Standard curves were obtained for each DNA preparation relating fully melted absorbances to DNA concentrations determined with diphenylamine, using calf thymus DNA as the chemical standard. Concentrations of DNA used in renaturation experiments were determined with these standard curves and the very precisely measured absorbances at 260 nm of the fully melted DNA sample used in the experiment. This procedure avoids the high errors (± 5%) in determining each concentration of renaturing DNA by the chemical method. The conversion factor between DNA concentration and absorbance at 260 nm of the fully melted DNA varied only slightly (less than 5%) from sample to sample, averaging to about 5.40×10^{-5} M base pairs for a fully melted absorbance at 260 nm of 1.0 in a 10 nm pathlength cuvette.

3.3. DNA shearing

Purified DNA samples in 1 X SSC buffer and flushed with nitrogen were sheared at about 0°C (on ice)

using a Bronson Power Sonifier, Model W185, at 65 watts (pre-calibrated against 1 × SSC buffer). The samples were given three 30 second sonication treatments, separated by one minute intervals.

Molecular weights of single stranded, sheared DNA samples at pH 13 were determined by sedimentation in an analytical Spinco Model E ultracentrifuge [12]. The sonication method discussed above for shearing purified DNA samples gave reasonably reproducible single strand molecular weights. For this study, the average single strand fragment size is 1250 ± 150 nucleotides ($4.15 \pm 0.50 \times 10^5$ daltons).

3.4. Renaturation

Sonicated DNA samples were adjusted to the salt concentrations to be used in the experiments by dialysis against a large excess of 0.02 M phosphate buffer (equimolar quantities of Na_2HPO_4 and NaH_2PO_4) with enough added NaCl to bring the final Na^+ concentration up to the desired level. Renaturation reactions were monitored by following the decrease in absorbance at 260 nm with an Automatic Recording Gilford Spectrophotometer, Model 2000, equipped with an automatic reference compensator, a circulating constant temperature water bath, a linear temperature programmer and a sample chamber temperature probe. The DNA samples were first denatured by heating at 100°C for 8 minutes in a Labline Temp-Block. The cuvettes were then quickly transferred to the sample chamber of the Gilford spectrophotometer (preheated to the renaturation temperature) and recording begun. Using a thermistor dipping into a 10 mm pathlength cuvette, the temperature equilibrium time after transfer was determined to be one to two minutes. At the conclusion of most renaturation experiments, the DNA samples were melted and absorbances at 260 nm obtained.

3.5. Data analysis

Reciprocal second-order (RSO) plots were constructed from the experimental data by the method described by Wetmur and Davidson [6], using the hyperchromicity of the native, unsheared DNA. The hyperchromicity of unsheared DNA is used rather than that for sheared DNA since it has been demonstrated that shearing can reduce the hyperchromicity of DNA and, furthermore, that DNA strands can renature to a greater extent than predicted by the sheared hyperchromicity [1]. Presumably, this phenomenon is caused by the formation of single-stranded ends on the double-stranded DNA as a result of shearing. Rate constants of renaturation can either be extracted from the initial RSO slopes of the second-order reaction or from the half-times of reaction.

For any optically monitored renaturation experiment, after transferring the denatured DNA to renaturing temperature there is observed an initial, rapid decrease in absorbance at 260 nm. The total magnitude of this decrease is dependent on salt and temperature conditions, but is independent (± 5%) of DNA concentration when expressed on a fraction of total reaction basis. The approximate half time of this reaction (about 2–3 min) is independent of DNA concentration, i.e., the reaction appears to be first-order. This phenomenon is observed by most researchers reporting optical renaturation data in the literature and is considered to be due to the formation of single strand structure. In 0.4 M Na^+, at $T_m - 25$°C, about 10% of the total absorbance change for complete reaction is due to single strand structure formation. Fig. 2 shows an RSO plot uncorrected for this single strand structure formation for the renaturation of E. coli DNA in 0.4 M Na^+, at 60°C. The intercept of the extrapolation of the linear portion of the initial second-order part of reaction with the ordinate axis $(A_0/A(t) - 1)$ at $t = 0$ enables one to calculate the fraction of the total absorbance change that corresponds to the second-order renaturation reaction (as determined by concentration dependence) and, conversely, the fraction that corresponds to the first-order reaction.

To obtain renaturation RSO data that reflects only the fraction of the total absorbance change that corresponds to the second-order renaturation reaction, the contribution to the absorbance change from single strand structure formation must be "subtracted" from the apparent fraction of reaction (on an absorbance basis) obtained from the raw (uncorrected) renaturation data at any time. If we let $(A(t)/A_0)_{uncor}$ denote the apparent fraction of unreacted nucleotides at time t, calculated from the raw data (containing both the first and second-order reaction components), $(A(t)/A_0)_{cor}$ denote the fraction of nucleotides at time t that are not in two stranded helical segments, i.e., the fraction of nucleotides that have not under-

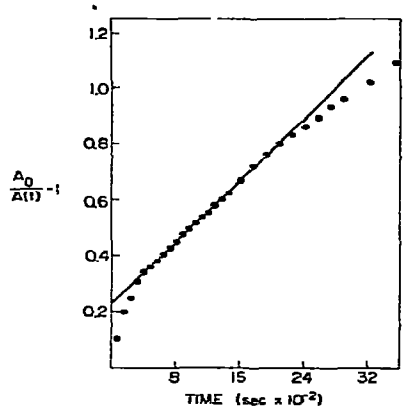

Fig. 2. Raw experimental RSO data, i.e., uncorrected for single strand structures, for the renaturation of E. coli DNA (A_0 = 2.38 × 10^{-4} M base pairs), in 0.4 M Na^+, at 60°C is shown to illustrate the effect of single strand structure formation. The straight line is an extrapolation of the initial linearity of the data for the second-order renaturation reaction. From the intercept of this line (0.23) at time t = 0, the fraction of the total reaction that is second-order renaturation is calculated to be about 0.81 (= 1/1.23).

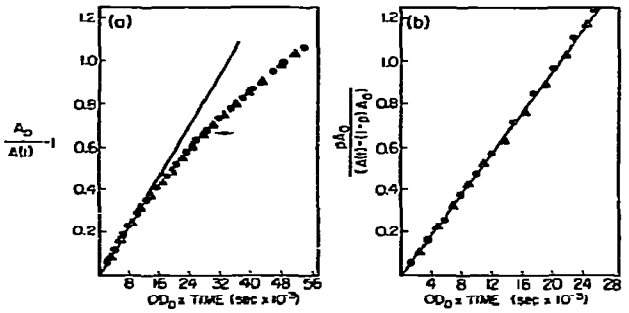

Fig. 3. (a) Concentration normalized RSO graphs for the renaturation of two concentration of E. coli DNA in 0.2 M Na^+, at 70°C. ▲ A_0 = 2.30 × 10^{-4} M base pairs, ● A_0 = 8.97 × 10^{-5} M base pairs. The straight line is the extrapolation of the early time slope of the data. The slopes of these lines are used in calculating the experimental second-order rate constants. As reference, half-reaction is at $A_0/A(t) - 1 = 1$, and 40% reaction is at $A_0/A(t) - 1 = 0.667$ (indicated by the arrow). (b) The kinetic data of fig. 3a is recalculated according to the modified RSO relationship [4], with $\alpha = p = 0.70$ and shown on a concentration normalized time scale. ▲ A_0 = 2.30 × 10^{-4} M, ● A_0 = 8.97 × 10^{-5} M.

gone a second-order renaturation reaction, and let q denote the fraction of the total absorbance changes that corresponds to the second order renaturation, then it can be shown [13] that

$$\left(\frac{A(t)}{A_0}\right)_{cor} = \frac{1}{q}\left(\frac{A(t)}{A_0}\right)_{uncor}. \quad (8)$$

This procedure is strictly analogous to that used in correcting hydroxyapatite data for zero-time-binding [14]. A modified form of this procedure has also been used for optical renaturation experiments [5]. Values of p calculated from experimental data must also be corrected for single strand structures in order to accurately reflect only the second-order part of the reaction. The necessary correction is given by

$$p_{cor} = p_{uncor}/q. \quad (9)$$

4. Results

As an example of nucleation rate-limited kinetics, fig. 3a shows concentration normalized (time scale A_0t instead of t) RSO plots for the renaturation of E. coli DNA in 0.2 M Na^+, at 70°C, at two concentrations. As is the case with renaturation experiments monitored with S1 nuclease [2,3], there is apparent substantial deviation from ideal (linear) second-order kinetics. The second-order rate constants, determined from the initial slopes of the curves, are, however, well within experimental error for the two concentrations (k_2 = 0.56 $M^{-1}s^{-1}$ for both concentrations, A_0 = 2.30 × 10^{-4} M base pairs and A_0 = 8.97 × 10^{-5} M). One can observe that the curvatures for the two concentrations are well within experimental error of being identical. Our operational definition of nucleation rate limiting kinetics is that both k_2 and the amount of curvature are independent of DNA concentration (see discussion).

For some early time portion of the reaction, the curvature can be quantitated by determining the best fit value of p in eq. (7). This can be accomplished in two ways: Using eq. (4) with p substituted for α and then finding the value of p which best linearized the data when the left hand size of eq. (4) is plotted against time. The second method in which p can be determined directly involves taking the first derivative of the $A(t)$ versus t experimental data and using the following equation which can be derived from eq. (7)

$$\left[\frac{A'(t)}{A_0}\right]^{-1/2} = \left[\frac{1}{p k_2 A_0}\right]^{1/2} + \left[\frac{k_2 A_0}{p}\right]^{1/2} t, \qquad (10)$$

where $A'(t) = dA(t)/dt$. Therefore, if experimental data is plotted at the left hand side of the above equation against time, the result will be a straight line for those portions of the reaction that can be characterized by a single value of p and k_2 (in practice, about the first 40% reaction). Additionally, the inverse of the product of the slope and intercept yields the value of p. This method has the additional advantage that the infinity point of the reaction OD(∞), need not be known to determine $A'(t)$. Thus, errors in curvature due to picking the wrong infinity point are eliminated. Further details and discussion of this method may be found in Rau [13].

For the E. coli data in fig. 3a, the best fit value of p is 0.70 as determined by the derivative method. With this value of p, the kinetic data can be linearized for the first 40% of the reaction if plotted according to the modified RSO relationship derived earlier, eq. (4) (with p substituted for α). Fig. 3b shows the resultant modified RSO plots (concentration normalized) for the two concentrations. As expected, the data is well linearized.

It might be argued, however, that the observed deviations from ideal second-order kinetics for E. coli DNA renaturation are due to some peculiarity of the E. coli DNA, e.g., the result of isolating replicating E. coli chromosomes, yielding a DNA sample with more than one copy of some of the DNA. For this reason, T2, T4, T5 and B. subtilis were studied under nucleation rate-limiting conditions. In fig. 4a, concentration normalized RSO data is shown for two concentrations of T2 DNA, renaturing in 0.1 M Na^+, at 60°C. For comparison, E. coli DNA renaturation data, in 0.2 M Na^+, 70°C, is included (after normalizing the time axis for second-order rate constant and DNA concentration differences). As can be observed, not only are the initially determined second-order rate constants for the two T2 DNA concentrations within experimental error of one another, but also the curvatures of the RSO data are coincident for all three experiments (the E. coli DNA renaturation, and the two T2 DNA renaturations), within experimental error.

In fig. 4b, the kinetic data is now replotted according to a normalized form of the modified RSO relationship, eq. (4), with $p = 0.71$ substituted for α showing that the data can indeed be linearized with this value of p.

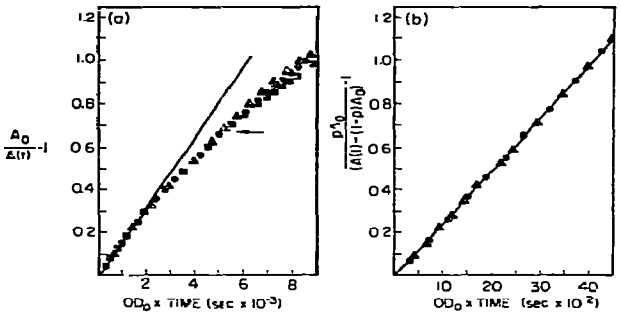

Fig. 4. (a) Kinetic data for the renaturation of T2 DNA in 0.1 M Na^+, at 60°C, is graphed according to a standard RSO relationship with a concentration normalized time axis. Dat.. for E. coli DNA, renaturing in 0.2 M Na^+, at 70°C, is included. The time axis for the E. coli DNA reaction is rate normalized, i.e., the time scale is (k_2, E. coli/k_2, T2) $OD_0 t$. • T2DNA A_0 = 4.37×10^{-5} M base pairs. ▲ T2DNA A_0 = 1.69×10^{-4} M base pairs, ▪ E. coli DNA A_0 = 2.30×10^{-4} M base pairs. The arrow indicates the 40% reaction point ($A_0/A(t) - 1 = 0.667$). (b) The kinetic data of fig. 4a replotted according to the modified RSO relationship, (4), with $p = 0.71$. • T2 DNA, $A_0 = 4.37 \times 10^{-5}$ M, ▲ T2 DNA, $A_0 = 1.69 \times 10^{-4}$ M.

A summary of kinetic data for E. coli DNA renaturation experiments in 0.1 M Na^+, 0.2 M Na^+ at about $T_m - 20$°C, and in 0.4 M Na^+ at 80°C ($T_m - 15$°C), is given in table 1. A summary for T2 DNA is presented in table 2. As can be noted, the initially observed second-order rate constants for a given set of renaturation conditions, are all within experimental error (5%) for the concentration range studied. The same can also be observed for rate constants determined from half-times of reaction. Furthermore, not only are the deviations from ideal second-order kinetics (as quantitated by p) independent of DNA concentration, but also the curvature is described by the same value of p for all the salt and temperature conditions studied here that give nucleation rate-limited kinetics. For these experimental conditions, $p \approx 0.70 \pm 0.01$.

In addition to the T2 and E. coli DNA results reported here, essentially identical results have been obtained for extensive experiments on T4, T5 and B. subtilis DNA under nucleation rate limiting conditions [13]. Values of k_2 for any given DNA sample renaturing in a particular set of salt and temperature conditions are, within experimental error, independent of DNA concen-

Table 1
A summary of the kinetic data for the renaturation of E. coli DNA at several concentrations is given for three different salt and temperature conditions that yield nucleation rate-limited kinetics. Values of k_2, observed second-order rate constants, were determined from the initial slopes of RSO curves. Values of $1/A_0t_{1/2}$ are the rates constants determined from half-times of reaction. Values of p were determined as described in the text. Values of k_2 and p given in the table are the averages from at least triplicate experiments.

A_0 (M base pairs)	k_2 ($M^{-1}s^{-1}$)	$1/A_0t_{1/2}$ ($M^{-1}s^{-1}$)	p
0.1 M Na^+, 65°C			
2.62×10^{-4}	0.17 ± 0.02	0.11 ± 0.01	0.71 ± 0.01
1.76×10^{-4}	0.15 ± 0.02	0.09 ± 0.02	0.70 ± 0.01
9.86×10^{-5}	0.14 ± 0.01	0.10 ± 0.01	0.70 ± 0.01
0.2 M Na^+, 70°C			
2.34×10^{-4}	0.57 ± 0.02	0.37 ± 0.02	0.70 ± 0.02
1.73×10^{-4}	0.55 ± 0.03	0.37 ± 0.03	0.70 ± 0.01
9.03×10^{-5}	0.56 ± 0.02	0.36 ± 0.03	0.71 ± 0.01
7.05×10^{-5}	0.54 ± 0.03	0.38 ± 0.02	0.69 ± 0.01
5.37×10^{-5}	0.55 ± 0.02	0.37 ± 0.03	0.70 ± 0.01
0.4 M Na^+, 80°C			
2.29×10^{-4}	1.24 ± 0.07	0.83 ± 0.05	0.71 ± 0.01
1.76×10^{-4}	1.21 ± 0.06	0.80 ± 0.08	0.70 ± 0.01
9.84×10^{-5}	1.22 ± 0.08	0.81 ± 0.06	0.71 ± 0.01
7.17×10^{-5}	1.20 ± 0.04	0.74 ± 0.05	0.69 ± 0.01
5.33×10^{-5}	1.25 ± 0.05	0.83 ± 0.07	0.70 ± 0.01

Table 2
A summary of kinetic data for the renaturation of T2 DNA is given for several different DNA concentrations renaturing in two different salt and temperature conditions that yield nucleation rate-limited (DNA concentration independent) second-order kinetic parameters. Values of k_2 were determined from the initial slopes of RSO curves. Values of $1/A_0t_{1/2}$ are the rate constants determined from half-times of reaction. Values of p were determined as described in the text. Values of k_2 and p for each DNA concentration are the average from at least triplicate experiments

A_0 (M base pairs)	k_2 ($M^{-1}s^{-1}$)	$1/A_0t_{1/2}$ ($M^{-1}s^{-1}$)	p
0.1 M Na^+, 60°C			
1.73×10^{-4}	2.87 ± 0.06	1.91 ± 0.05	0.71 ± 0.01
9.06×10^{-5}	3.04 ± 0.07	2.03 ± 0.08	0.71 ± 0.01
7.02×10^{-5}	2.92 ± 0.05	1.99 ± 0.06	0.72 ± 0.01
3.46×10^{-5}	3.01 ± 0.06	1.97 ± 0.04	0.70 ± 0.01
0.2 M Na^+, 65°C			
1.65×10^{-4}	10.4 ± 0.4	7.05 ± 0.32	0.70 ± 0.01
9.72×10^{-5}	10.8 ± 0.3	7.13 ± 0.45	0.71 ± 0.01
4.83×10^{-5}	10.4 ± 0.3	7.12 ± 0.45	0.71 ± 0.01

tration in the approximate range of 9×10^{-5} to 3×10^{-4} M base pairs. Furthermore, p values for all DNA samples, renaturing in any set of nucleation rate-limiting salt and temperature conditions, are constant for the first 40% of reaction, with a value of 0.70.

It must be concluded from these results that the observed deviation from ideal second-order kinetics is not due to some anomalous peculiarity of a particular DNA sample, but is a general feature of the renaturation of randomly sheared DNA. This is the same conclusion reached by Morrow [3] in examining S1 nuclease monitored kinetics for randomly sheared DNA samples from SV40, ϕ X 174RF, M13RF and E. coli.

5. Discussion

While the ideal theory presented here does indeed explain satisfactorily the difference in RSO curvature between hydroxyapatite monitored experiments and optical density or S1 nuclease monitored experiments, the almost quantitative agreement for curvature is surprising (p = 1.0 for hydroxyapatite, compared to the ideal value of 1.0 and p = 0.7 which is close to the ideal value of $\frac{2}{3}$ for optical experiments). This quantitative agreement is most likely a near cancelling of opposite effects on curvature which we now discuss.

5.1. Reactions of single-strand ends on partially base-paired two stranded species.

The reaction of the free ends of partially base-paired species with free single strands can be analyzed analytically for the reaction of two stranded species with a free single strand to form three-stranded species. Miller and Wetmur [15] have reported that one does not observe significant quantities of three stranded partially helical species in the reaction mixture until about 40–50% reaction. It seems, therefore, that up to 40% reaction, it is a very reasonable assumption to exclude from kinetic analysis all reactions yielding four (or more) stranded partially helical species.

The sequence of reactions to be considered is schematically represented in fig. 5. The kinetic equations for these reactions are given by,

$$d R(t)/dt = -k_2 R^2(t) - \tfrac{1}{2} k_3 R(t) S(t) \quad (11)$$

$$d S(t)/dt = k_2 R^2(t) - k_3 R(t) S(t)$$

$$d U(t)/dt = k_3 R(t) S(t),$$

with the constraint that at any time t, $R(t) + S(t) + \frac{3}{2} U(t) = R_0$, where, as previously, $R(t)$ is the concentration of either (+) or (−) strands, $S(t)$ and $U(t)$ are the concentrations of whole species (S and U, respectively) at time t. The second-order rate constants, k_2 and k_3, are the rate constants for the reaction of whole species. If a fraction α of the total number of base pairs zip following the successful nucleation of two free single strands of length L, then k_2 and k_3 can be expressed in terms of the nucleation rate constants per nucleotide, k_2^0 and k_3^0, respectively, by

$$k_2 = L k_2^0,$$

and

$$k_3 = 2(1-\alpha) L k_3^0.$$

The solution of the kinetic equations shown above is complex and presented in Rau [13]. The final equation for $A_0/A(t) - 1$ involves among other terms, an integral which must be evaluated numerically, so the equation does not have the simple form of eqs. (4)–(7). However, the equation still predicts downward curving RSO plots, and, in fact, its time course near $t = 0$ can be well approximated by the simple empirical relationship for RSO curvature, eq. (7). Thus, Rau [13] could relate the empirical measure of curvature, p, at zero time to α, k_2^0 and k_3^0. The resulting relationship is

$$p(t=0) = \alpha \left(1 - \frac{(1-\alpha)^2}{\alpha} \frac{k_3^0}{k_2^0}\right)^{-1}. \quad (12)$$

Using this equation, we can predict approximately the effect on curvature of the reaction of single-strand ends on two-stranded species to form three-stranded species. As an example, let $\alpha = \frac{2}{3}$ (the ideal value) and let $k_3^0/k_2^0 = \frac{1}{3}$. (Britten et al. [2] have found experimentally that $k_3^0/k_2^0 = \frac{1}{2}$ to $\frac{1}{4}$). Using these values, eq. (12) gives $p = 0.71$. Thus, the curvature has *decreased* ($\Delta p = +0.04$) due to the reaction of single strand ends.

One might guess that once all the reactions of ends to form 3, 4, 5, ...-stranded species are taken into account that the kinetics will then become ideal second-order ($p = 1$). This is not the case. Rau [13] was able to write down the set of differential equations for the formation of 3, 4, 5,...-stranded species. While these equations are much too difficult to solve, we could at least ask the question "What condition is necessary and sufficient for the set of equations to collapse into a single, ideal second-order differential equation?" The condition is that the nucleation rate constant per nucleotide for forming an i stranded species from any other two species, k_i^0, times the number of base pairs which zip up, α_i, must be a constant. In symbols, $\alpha_2 k_2^0 = \alpha_3 k_3^0 = \alpha_4 k_4^0 = \ldots$. Since less base pairs zip up when a free single strand end of a partially base-paired species reacts than when two free single strands react and since it has been empirically found [2] that the nucleation rate constant $k_3^0 < k_2^0$, the condition for ideal second-order kinetics is far from realized in practice. Thus, S1 or optically monitored reactions will show downward curving RSO plots under nucleation rate-limiting conditions. The exact amount of curvature cannot be approximated except for the first 40% of reaction where it is reasonable to assume only two and three stranded species form. Under these conditions, $\Delta p = +0.03$ to $+0.15$ is a reasonable, wide range of probable values.

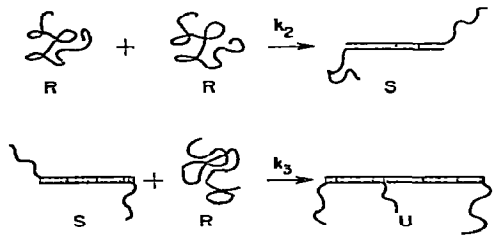

Fig. 5. A schematic representation of the two consecutive reactions to be considered (1), the reaction of two free single strands with a second-order nucleation rate constant k_2 and (2), the reaction of a free single strand and a tail of a partially helical duplex, with a nucleation rate constant k_3.

The equation of Morrow [3] also describes downward curving RSO plots quite well. However, the physical interpretation of that theory is different from ours. We first summarize the Morrow theory and then discuss the differences.

The Morrow approach assumes that there are apparently decreasing rate constants of renaturation, $k_2(t)$ (as inferred from the downward curvature of RSO plots) and that they can be simply related to the fraction unreacted by the relationship,

$$k_2(t) = k_2(t=0)[A(t)/A_0]^x. \quad (13)$$

For this model, the second order rate equation takes the form,

$$-\frac{dA(t)}{dt} = k_2(t)A^2(t) = \frac{k_2(t=0)}{A_0^x}A^{(2+x)}(t). \quad (14)$$

When integrated this yields the modified second-order relationship

$$\frac{A(t)}{A_0} = \left[1 + \frac{k_2(t=0)}{N}A_0 t\right]^{-N}. \quad (15)$$

where $N = 1/(1+x)$. With a value of $N = 0.44$, this equation describes quite well S1 and optically monitored kinetics under nucleation rate limiting conditions.

Our physical interpretation of this equation is that it predicts ideal second-order kinetics at $t = 0$ and that *downward curvature of RSO plots is produced at $t > 0$ by the slower reactions (in terms of rate constants) of the single-strand ends* of partially base-paired species. In a sense, this is exactly opposite our explanation which says that *the first early-time event produces downward curvature* in RSO plots since $\alpha = \frac{2}{3}$ (for the ideal case), and that *the later reactions of single strand ends tend to reduce the curvature.* As a practical tool for linearizing RSO plots to extract rate constants eq. (15) is as good, or even slightly better, than eq. (7) since it linearizes data well past 40% reaction.

The theory of Britten and Davidson [16] is similar to that of Morrow [3], so that the physical interpretation of their theory differs in much the same way from ours as does Morrow's. Also, Miller and Wetmur's [15] result that single strand ends do not react significantly before 40% reaction, would lead to a prediction of linear RSO plots up to 40% reaction using these [3,16] theories.

5.2. Effect of distribution of single-strand lengths on curvature.

There are two effects due to a length distribution of single strands. The first is that the average number of base pairs formed when two single strands react is reduced from the ideal $\alpha = \frac{2}{3}$ value. While the exact value of α depends on the actual single strand length distribution, Miller and Wetmur [15] have shown that for a typical distribution $\alpha \approx 0.6$. Thus, the effect is to *increase* curvature of RSO plots ($\Delta p = -0.07$ from the ideal case).

The second effect of a single-strand length distribution on curvature is that longer strands will tend to react faster than shorter strands (since k_2 increases as L increases [6]) thereby increasing RSO curvature (Δp negative). We have been unable to quantitate this effect even approximately for a realistic case because too many inaccurate assumptions must be made.

5.3. Effect of non-homogeneous base composition

If some of the sheared single strands have a higher G + C content than others, they might be expected to renature faster causing more curvature in RSO plots (Δp negative). This effect cannot be quantitated without a detailed knowledge of the base composition of the strands. For simple DNA, such as that from bacteria or bacteriophage, it is generally assumed that these effects are minimal. From the quantitative agreement for curvature of our experiments on T2, T4, T5, B subtilis and E. coli DNA, we can conclude that the effect of G + C heterogeneity is at least constant, if not absent.

5.4 Summary

We have discussed above the major factors affecting curvature of RSO plots of DNA renaturations. For hydroxyapatite monitored kinetics it is experimentally observed that the kinetics follow a nearly ideal second-order time course ([1,2] and our own unpublished observations); that is, $p \approx 1$. This conforms to the ideal case theory presented here, where $p = 1$ is the expected value for hydroxyapatite experiments. The experiments presented here for optical density and those of Morrow [3] for S1 nuclease are well linearized with $p = 0.7$ which is very close to the ideal value $p = \frac{2}{3}$. Because of this surprising agreement with the ideal case, we can only conclude that the other factors affecting curvature (reaction of single strand ends, length distribution of single strands, and G + C heterogeneity in single strands – all of which should effect curvature of hydroxyapatite, optical density and S1 experiments to nearly the same extent) are such that they fortuitously nearly cancel. Specifically, the reaction of single-stranded ends which *decreases* curvature must nearly cancel the other effects which

increase curvature, so that almost "ideal" kinetics result.

The optical density monitored experiments presented here on E. coli and T2 DNA and others on B. subtilis, T5 and T4 DNA (not presented, but extensively carried out) show quantitatively the same downward curving RSO plots under nucleation rate limiting conditions. We conclude that this curvature is probably not a peculiarity of the DNA's studied but likely holds for most simple DNA.

We have been careful to include the qualification, nucleation rate limiting conditions, when discussing data here. Our operational definition of nucleation rate limiting conditions is: certain salt and temperature conditions that yield a time course description of the kinetics and second-order rate constants that are independent of DNA concentration. That such conditions hold for our experiments is documented in tables 1 and 2. The reason for adopting such a peculiar definition for nucleation rate limiting conditions is that there exist high salt and low temperature conditions in which not only are second-order rate constants DNA concentration dependent, but also the time course description of the kinetics (curvature) varies with DNA concentration [13,17]. Specifically, p increases with increasing DNA concentration until the kinetics at times can appear to be ideal second-order ($p \approx 1$). However, under those conditions the rate constants are quite concentration dependent, decreasing with increasing DNA concentration. A theory has been developed [17] that can well explain this apparently anomalous kinetic behavior. The theory is based on the idea that zipping is slowed due to formation of secondary structures in the single strands under high $[Na^+]$, low temperature conditions. Whatever the cause of concentration dependent rate constants and curvature, it is clearly important to choose conditions where they are not. We find $[Na^+] \leqslant 0.2$ M, renaturation temperatures closer to T_m than $T_m - 25°C$ and low DNA concentration to be such conditions for DNA of sequence complexity comparable to bacteria.

In conclusion, while the theory presented in this paper may not be of more practical importance than others [3,16] for the purpose of extracting rate constants to obtain DNA sequence complexities, the theory presents, in our view, a more physically correct description of DNA renaturation and thus provides a better "jumping-off" point for more detailed theories.

Acknowledgements

We wish to acknowledge stimulating discussions with Dr. Hans Lehrach. We wish to thank Alan Hinnebusch and Dr. Thomas Roberts for useful suggestions concerning the manuscript.

The research was supported by both NSF Grant PCM-11158 and NIH Grant GM-20798.

References

[1] R.J. Britten and D.E. Kohne, Carnegie Inst. Was. Year Book 65 (1967) 78.
[2] M.J. Smith, R.J. Britten and E.H. Davidson, Proc. Natl. Acad. Sci. 72 (1975) 4805.
[3] J. Morrow, Ph. D. Thesis, Stanford University (1974).
[4] M. Gillis, J. Deley and M. DeCleene, Eur. J. Biochem. 12 (1970) 143.
[5] C. Christiansen, G. Christiansen and A.L. Bak, J. Mol. Biol. 84 (1974) 65.
[6] J.G. Wetmur and N. Davidson, J. Mol. Biol. 31 (1968) 349.
[7] J.G. Wetmur, Ph. D. Thesis, California Institute of Technology (1967).
[8] L.C. Klotz and A. Hinnebusch, unpublished results.
[9] J. Marmur, J. Mol. Biol. 3 (1961) 208.
[10] C.A. Thomas Jr. and J. Abelson, in: Procedures in nucleic acid research, eds. G.C. Cantoni and D.R. Davies (Harper and Row Publishers, New York, 1966) p. 553.
[11] J.M. Kissane and E. Robins, J. Biol. Chem. 233 (1958) 184.
[12] F.W. Studier, J. Mol. Biol. 11 (1965) 373.
[13] D.C. Rau, Ph. D. Thesis, Harvard University (1975).
[14] E.H. Davidson, B.R. Hough, C.S. Amenson and R.J. Britten, J. Mol. Biol. 77 (1973) 1.
[15] S.J. Miller and J.G. Wetmur, Biopolymers 14 (1975) 309.
[16] R.J. Britten and E.H. Davidson, Proc. Natl. Acad. Sci. 73 (1976) 415.
[17] D.C. Rau and L.C. Klotz, J. Chem. Phys. 62 (1975) 2354.
[18] R.B. Roberts, P.H. Abelson, D.B. Cowie, E.J. Bolton and R.J. Britten, Carnegie Institute of Washington Publication, 607, Washington, D.C. 5 (1955).